frontiers | Frontiers in Energy Research

TYPE Original Research
PUBLISHED 13 February 2024
DOI 10.3389/fenrg.2024.1352540

OPEN ACCESS

EDITED BY
Jiawei Wang,
Technical University of Denmark, Denmark

REVIEWED BY
Hamid Reza Rahbari,
Aalborg University, Denmark
Mohamed Salem,
University of Science Malaysia (USM), Malaysia

*CORRESPONDENCE
Chuang Zhu,
zzccpy_22@163.com

RECEIVED 08 December 2023
ACCEPTED 26 January 2024
PUBLISHED 13 February 2024

CITATION
Wang K, Chen L, Li X and Zhu C (2024), Research on compressed air energy storage systems using cascade phase-change technology for matching fluctuating wind power generation. *Front. Energy Res.* 12:1352540.
doi: 10.3389/fenrg.2024.1352540

Research on compressed air energy storage systems using cascade phase-change technology for matching fluctuating wind power generation

Kangxiang Wang[1], Laijun Chen[1,2], Xiaozhu Li[2] and Chuang Zhu[1]*

[1]College of Energy and Electrical Engineering, Qinghai University, Xining, China, [2]Department of Electrical Engineering and Applied Electronics Technology, Tsinghua University, Beijing, China

The wind speed varies randomly over a wide range, causing the output wind power to fluctuate in large amplitude. An isobaric adiabatic compressed air energy storage system using a cascade of phase-change materials (CPCM-IA-CAES) is proposed to cope with the problem of large fluctuations in wind farm output power. When the input power is lower than the minimum energy storage power of the compressor, the gradient phase-change thermal energy storage is utilized to broaden the operating range of the system. Second, the system design method and operation rules are elaborated. The storage/release characteristic curve is obtained by constructing the system components and the overall variable operating condition model. A matching system scheme is designed according to the characteristics of a wind farm in a port in China. The case study shows that the wind farm configured with the CPCM-IA-CAES system reduces the wind abandonment rate by 5.7%, recovers 4,644.46 kW h of wind power abandonment, and improves the storage power index by 16.67% compared with that of IA-CAES. Meanwhile, the system efficiency is increased from 65.96% to 74.68%, and the energy storage density is increased from 8.69 to 9.89 kW h m^{-3}.

KEYWORDS

cascade phase-change energy storage, compressed air energy storage, operating mode, thermal cycle, wind power

1 Introduction

The increasingly severe global environmental and climate change challenges have made most countries and regions focus on sustainable development and the efficient use of renewable energy (Erdiwansyah et al., 2021). It has gradually become a consensus to achieve a high proportion of renewable energy in the power supply (Yang et al., 2021). The European Union, the United States, and China have proposed to achieve 100%, 80%, and 60% renewable energy power supply plans by 2050, respectively (Zhou et al., 2022). New energy will occupy an increasing proportion of the Chinese energy consumption structure (Olujobi, 2020). However, due to the intermittent and random characteristics of new energy (Xuezhao et al., 2023), such as its large-scale access to the power grid (Xu et al., 2012), it will

have a great impact on the safe and stable operation of the power grid (Yang et al., 2022c) and its power quality (Yang et al., 2022b).

Large-scale energy storage (power storage and heat storage) technology is one of the main measures to smooth the fluctuations in the new energy output (Mei et al., 2018). According to different principles, energy storage technology can be divided into pumped storage (Xu et al., 2023), compressed air energy storage, phase-change energy storage, and flywheel energy storage (Luo et al., 2015). Among them, compressed air energy storage (CAES) has attracted the attention of many large enterprises (Li et al., 2023b) and research institutions at home and abroad due to its advantages of large capacity, long life, and fast response speed (Budt et al., 2016). Isobaric adiabatic compressed air energy storage (IA-CAES) has become a promising energy storage system due to its technical advantage of constant pressure in the air storage reservoir (Wang et al., 2016b). Nevertheless, the current IA-CAES system has its limitations (Tessier et al., 2016): 1) from the perspective of system energy loss, the heat generated during the compression process in the storage and heat exchange processes inevitably exists and is difficult to fully utilize, resulting in the IA-CAES cycle efficiency not being high and the gap between the ideal storage efficiency of 90% being large (Tong et al., 2021); 2) from the perspective of the system operating under variable conditions, the compressor is subjected to the constraints of surging margins; the choking margins need to be set for the minimum and maximum pressures; and when the input power exceeds these constraints, the operating efficiency and lifespan of the system are significantly reduced (Shafiee et al., 2018). In this regard, a number of scholars have carried out research on this issue and obtained many results. In terms of variable operating conditions, Arabkoohsar et al. (2020) proposed that the overall performance efficiency of cryogenic compressed air energy storage systems is affected by partial load conditions. The results show that at 50% load, system efficiency is 52%, and at 10% load, system efficiency is only 28%. Shang et al. (2020) proposed the effect of variable operating conditions on the efficiency and economy of a cryogenic adiabatic compressed air energy storage system. The results show that system efficiency at 30% load is much lower than that at the rated condition, and the payback period at the non-rated condition is much higher than that at the rated condition. Rahbari and Arabkoohsar (2021) thoroughly investigated the performance of multi-energy interconnected energy storage systems under variable-condition operation. The results show that non-rated condition operation has a great negative impact on system efficiency, exergy parameters, and economy. In the case of compression heat recovery, Li et al. (2023a) proposed a coupled CAES system for thermal power units based on the thermodynamic model. The influence of key parameters on system performance is evaluated, and the results show that the efficiency of the coupling system can be increased by 16.21% and 5.39 tons of coal can be saved in a single cycle. Xiao et al. (2023) proposed a constant-pressure adiabatic compressed air energy storage system with work-heat storage. The system characteristics are obtained by constructing a model that accounts for variable conditions of the system, and the case study shows that the total released energy of the system increases by 52,137.07 MJ, and the wind curtailment rate decreases to 0.405%. Li et al. (2019) proposed a combined cooling, heating, and power system based on adiabatic compressed air energy storage; the system uses CAES, phase-change materials (PCMs), and water to store energy together. The performance of each component of the system is studied in detail by establishing a dynamic model of the system. The results show that the cycle efficiency can reach 96.56% under stable system operation conditions. Sciacovelli et al. (2017) proposed a CAES system coupled with packed-bed heat storage; the transient characteristics of the packed-bed heat storage system and compression/expansion system are described, and the results show that the efficiency of the coupling system is within 60%–70%. In summary, most of the existing studies on CAES systems focus on analyzing the effects of variable operating characteristics, yet no researcher has applied these characteristics to the design of energy storage devices. In addition, current IA-CAES heat storage at all levels is mostly used after mixed storage in the heat storage device; this type of heat storage method simplifies the system process, but the loss of heat leads to low system efficiency. In addition, most of the existing studies use sensible heat storage materials to store heat through temperature changes, and the decrease in temperature during energy release leads to a decrease in system operation stability (He et al., 2019).

In view of the above defects, this paper, based on the criterion of "temperature counterpart, gradient utilization," starts from the coupling of the heat cycle, considers the design of a heat storage system, a typical pressurizer/turbine characteristic curve, and a typical constant-pressure storage device as the basis, adopts the modularized way of constructing, builds the system variable working condition model, and puts forward a type of cascade phase-change constant pressure adiabatic CAES heat and power cogeneration system design method along with its operational rules. The system realizes the following objectives: 1) expanding the range of energy storage power regulation through the joint operation of heat storage and air storage reservoirs; 2) maintaining the system's heat storage temperature and improving its operational stability through the configuration of the molten salt medium; 3) realizing "temperature counterpart" independent heat storage through the design of graded heat storage, thereby reducing the heat loss during operation and improving the system operation efficiency. In addition, the CPCM-IA-CAES system and the operation scheme of the harbor wind farm are studied, and the results show that the designed system can cope with the fluctuation of energy storage power on an hourly timescale and a 10 MW power scale and has the advantages of high storage density and high system efficiency, which can provide a novel perspective for the development of the subsequent IA-CAES system.

2 System description

In this paper, a combined heat and power system is proposed by integrating IA-CAES with a cascade phase-change energy storage system based on the basic principle of "temperature matching, cascade utilization," and its structural diagram is shown in Figure 1. Figure 1A shows the structure of the CAES system with

10.3389/fenrg.2024.1352540

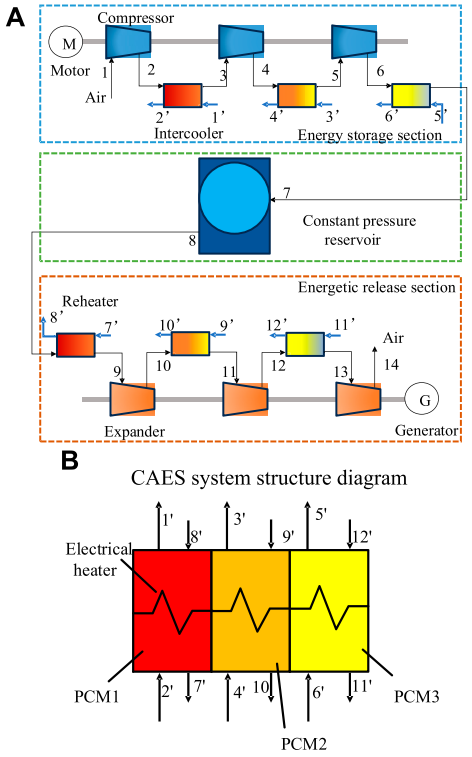

FIGURE 1
Structure diagram of the CAES system coupled with phase-change energy storage; **(A)** CAES system structure diagram and **(B)** Schematic diagram of cascade phase change energy storage system.

a constant-pressure air storage reservoir, and Figure 1B shows the structure of the phase-change energy storage system comprising multi-stage phase-change materials.

1) Energy storage stage: When the external input power is higher than the starting power of the compression section, the compression section compresses the air to a high pressure (energy flow of 1–7) and stores it in a constant-pressure air storage reservoir. At the same time, the compression heat is stored independently in three types of PCMs (energy flow from 1′ to 6′) using an three-stage intercooler. When the external input electric power is lower than the starting power of the compression section, the electric heater in the phase-change energy storage system starts and the electric power that should be discarded is collected and stored in the form of heat energy, and the compressor does not operate. When the external input electric power is higher than the maximum power of the compression section, the compressor and the electric heater operate simultaneously.
2) Energy release stage: The high-pressure air is discharged from the constant-pressure air storage reservoir at a constant pressure (energy flow is 8–14). In this process, the heat energy stored in the cascade phase-change energy storage is extracted from the three-stage reheater according to the corresponding temperature range, and the high-pressure air is heated. The air is discharged into the atmosphere after passing through the three-stage turbine. The waste heat after heat exchange in the cascade phase-change energy storage is used to heat the residents according to the principle of temperature matching to realize the efficient utilization of heat energy.

3 Thermodynamic model of the whole working condition of the system

3.1 Compressor

When the compressor is running, the power W_c and isentropic efficiency η_c are as follows (Nantian et al., 2020):

$$W_c = G_c\left(h_{2,c} - h_{1,c}\right),$$
$$\eta_c = \frac{h_{2,s,c} - h_{1,c}}{h_{2,c} - h_{1,c}}.$$

Here, the subscript c represents the compressor, 1 and 2 represent the inlet and outlet, respectively, and s represents the isentropic process. G_c represents the air mass flow rate of the compressor, kg/s; $h_{2,c}$ and $h_{1,c}$ represent the outlet-specific enthalpy and inlet-specific enthalpy of the compressor, respectively, kJ/kg; and $h_{2,s,c}$ represents the specific enthalpy of the working fluid when the isentropic process is compressed to the same outlet pressure, kJ/kg.

The function expressions of the pressure ratio and efficiency of the compressor with the change in the dimensionless flow rate and rotational speed (Zhang et al., 1996) under variable working conditions are as follows:

$$\frac{\pi_c}{\pi_{c0}} = c_1 m_c^{2'} + c_2 m_c^{'} + c_3,$$
$$\frac{\eta_c}{\eta_{c0}} = \left[1 - c_4\left(1 - n_c^{'}\right)\right]\left(\frac{n_c^{'}}{m_c^{'}}\right)\left(2 - \frac{n_c^{'}}{m_c^{'}}\right),$$
$$c_1 = \frac{n_c^{'}}{\left[p\left(1 - \frac{m}{n_c^{'}}\right) + n_c^{'}\left(n_c^{'} - m\right)^2\right]},$$
$$c_2 = \left(p - 2mn_c^{'}\right)^2\left[p\left(1 - m/n_c^{'}\right) + n_c^{'}\left(n_c^{'} - m\right)^2\right],$$
$$c_3 = -\frac{\left(pmn_c^{'} - m^2 n_c^{'} 3\right)}{\left[p\left(1 - \frac{m}{n_c^{'}}\right) + n_c^{'}\left(n_c^{'} - m\right)^2\right]},$$
$$c_4 = 0.3.$$

Here, π_c represents the pressure ratio; η_c stands for efficiency; $m_c^{'}$ represents the relative equivalent flow; $n_c^{'}$ represents the relative equivalent speed; the subscript c represents the compressor; and 0 indicates the design point. The expressions of $m_c^{'}$ and $n_c^{'}$ are as follows:

$$m_c^{'} = \frac{\left(\frac{m_c\sqrt{T_{c,in}}}{p_{c,in}}\right)}{\left(\frac{m_c\sqrt{T_{c,in}}}{p_{c,in}}\right)_0},$$
$$n_c^{'} = \frac{\left(\frac{n_c}{\sqrt{T_{c,in}}}\right)}{\left(\frac{n_c}{\sqrt{T_{c,in}}}\right)_0},$$

where $p_{c,in}$ represents the compressor inlet pressure, kPa; $T_{c,in}$ represents the inlet temperature of the compressor, K; p = 1.8; and m = 1.8.

3.2 Turbine

$$W_t = G_t(h_{2,t} - h_{1,t}),$$
$$\eta_t = \frac{h_{1,t} - h_{2,t}}{h_{1,t} - h_{2,s,t}}.$$

Here, the subscript t represents the air turbine; represents the air mass flow rate of the turbine, kg/s; $h_{1,t}$ and $h_{2,t}$ represent, respectively, the specific enthalpy of turbine inlet and outlet, kJ/kg; $h_{2,s,t}$ represents the outlet specific enthalpy of the turbine when it expands to the same outlet pressure according to the isentropic process, kJ/kg. The expansion ratio, initial temperature, flow rate, and other parameters meet the improved Flugel formula (Zhang and Cai 2002a) when the centrifugal turbine operates under variable working conditions as follows:

$$m_t' = \alpha\sqrt{T_{30}/T_3}\sqrt{(\pi_t^2 - 1)/(\pi_{t,0}^2 - 1)}.$$

Here, $\alpha = \sqrt{1.4 - 0.4n_t/n_{t,0}}$; T_3 represents the turbine's initial temperature; n_t represents the speed; π_t represents the expansion ratio; and the subscript 0 indicates the design condition.

The isentropic efficiency of a centrifugal turbine is calculated as follows:

$$\eta_t' = \left[1 - t_4\left(1 - n_t'\right)^2\right]\left(n_t'/m_t'\right)\left(2 - n_t'/m_t'\right).$$

3.3 Heat exchanger

Based on the temperature and pressure range that the high-pressure air in the system can reach, the heat exchanger selects the plate-fin heat exchanger. The basic relationship for the heat transfer calculation of a heat exchanger is as follows (Shu et al., 2014):

$$Q = UA\Delta T_m,$$
$$Q = m_h(i_{hi} - i_{ho}) = m_c(i_{co} - i_{ci}),$$
$$\Delta T = \frac{(\Delta T_{max} - \Delta T_{min})}{\left[\ln\left(\frac{\Delta T_{max}}{\Delta T_{min}}\right)\right]}.$$

Here(Ruiheng et al., 2023), Q stands for the heat transfer, kW; U is the average heat transfer coefficient of the whole heat transfer surface, kW/(m^2·K); A is the heat transfer area, m^2; ΔT_m is the logarithmic mean heat transfer temperature difference between the two fluids, K; ΔT_{max} is the large value of the end difference of the heat exchanger, K; ΔT_{min} is the small value of the end difference of the heat exchanger, K; m_h and m_c are, respectively, the mass flow rate of hot fluid and cold fluid, kg/s; i_{hi} and i_{ho} are the specific enthalpy of inlet and outlet of hot fluid, respectively, kJ/kg; i_{co} and i_{ci} are the specific enthalpy of cold fluid inlet and outlet, respectively, kJ/kg.

3.4 Air storage reservoir

The air storage reservoir includes an air pipeline for conveying compressed air and an underwater constant-pressure air storage reservoir. Since the air pipeline from the ground to underwater is sufficiently long, the heat exchange between the compressed air and the low-temperature deep seawater is sufficient during the air transportation process; it is considered that the storage temperature of the compressed air T_{as} is equal to the seawater temperature T_{sw}. At the same time, because the air storage reservoir is at a fixed seawater depth, the air storage pressure is a fixed value. Therefore, the air temperature $T_{a,out,as}$ and pressure $P_{a,out,as}$ at the outlet of the air storage tank can be expressed as follows (Yang et al., 2022a):

$$P_{a,out,as} = P_{as},$$
$$T_{a,out,as} = T_{as} = T_{sw}.$$

The mass change of compressed air in the air storage reservoir can be obtained according to the mass conservation equation as follows:

$$\frac{dM_{as}}{dt} = G_{a,in,as} - G_{a,out,as}.$$

In the type, $G_{a,in,as}$ and $G_{a,out,as}$ are the input and output air flow rates in the constant air storage reservoir, respectively.

3.5 Heat storage system

The following formula is used to calculate the temperature of a phase-change material in the sensible heat storage stage:

$$\frac{U}{I_{PCMs}}\left(T_{PCMs} - T_{TES\_PCMs,x}^{in}\right) = -\rho c_{p,PCMs}\frac{dT_{PCMs}}{dt}.$$

Here, I_{PCMs} represents the feature length, $T_{TES\_PCMs,x}^{in}$ indicates the inlet temperature in each compartment, T_{PCMs} represents the temperature, ρ represents the density, and $c_{p,PCMs}$ represents the specific heat capacity of the PCM.

For the latent heat storage stage, the temperature of the phase-change material remains almost unchanged. The energy stored in this stage is as follows:

$$m_{PCMs}Q_{lh} - Q_{rh} = \int_{0-tchar}\left(h_{TES_{PCMs},x}^{in} - h_{TES_{PCMs},x}^{out}\right)m_{dt}'dt,$$

where m_{PCMs} represents the mass; Q_{lh} represents the latent heat per kg of PCM; Q_{rh} represents the residual latent heat in the PCM; $h_{TES\_PCMs,x}^{in}$ represents the inlet entropy; and $h_{TES\_PCMs,x}^{out}$ represents the outlet entropy in each component.

3.6 Performance indicators

System efficiency $\eta_{CPCM-IA-CAES}$ is an important performance index to describe the energy utilization rate of an energy storage system. Energy storage density $E_{CPCM-IA-CAES}$ is an important index to measure the energy storage capacity of air storage reservoir. The mathematical description is as follows:

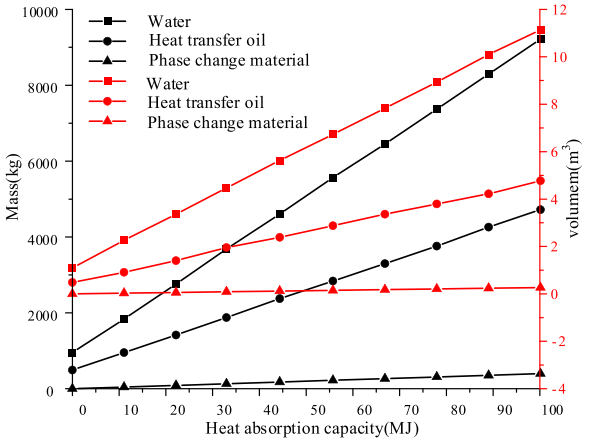

FIGURE 2
Effect of heat absorption on mass and volume for different thermal energy storage materials.

$$\eta_{\mathrm{CPCM-IA-CAES}} = \frac{E_{\mathrm{out}}}{E_{\mathrm{in}}} \times 100\%,$$

$$E_{\mathrm{CPCM-IA-CAES}} = \frac{E_{\mathrm{out}}}{V_{\mathrm{ac}}}.$$

Here, E_{out} represents the total electric energy released for the energy release process, kW·h; E_{in} represents the total electric energy consumed in the energy storage process, kW·h; V_{ac} represents the volume of the air storage reservoir, m^3.

The ability of different CAES systems to cope with fluctuating wind power inputs is expressed in terms of the storage power index W_{stor} as follows:

$$W_{\mathrm{stor}} = \frac{W_{\mathrm{H}} - W_{\mathrm{L}}}{W_{\mathrm{H}}} \times 100\%,$$

where W_{H} is the upper limit of energy storage power and W_{L} is the lower limit of energy storage power.

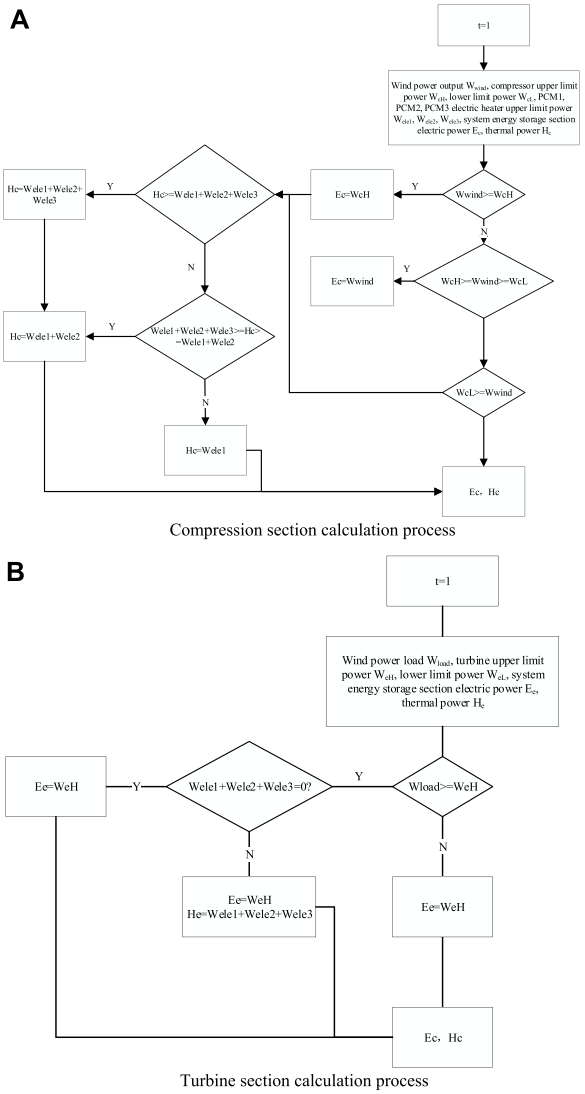

FIGURE 3
Flow chart of calculation; **(A)** Compression section calculation process and **(B)** Turbine section calculation process.

4 System key technology and operating mode

4.1 Key technologies of the system

For change materials and non-phase-change materials, the characteristics are shown in Figure 2. The temperature change in water and heat transfer oil is 5 K, and the phase-change temperature of the phase-change material is assumed to be in this range. By controlling the temperature range, all the phase-change materials are stored in the form of a phase change, and the temperature of the phase-change materials does not change in this process. It can be found that as the heat storage capacity increases, the amount of non-phase-change materials (water and heat transfer oil) required increases rapidly, while the phase-change materials hardly change. In the sensible heat storage stage, the temperature of the phase-change material (solid) increased with the absorption of heat. However, unlike traditional sensible heat storage materials, when the phase-transition temperature (melting temperature) is reached, the phase-change material absorbs a large amount of heat at an almost constant temperature, that is, during the latent heat storage phase (Mazloum et al., 2017).

In this paper, three types of phase-change materials with phase-change temperatures equal to the corresponding compressor outlet temperature are selected for the CPCM-IA-CAES system, as shown in Figure 1B. Each material is separated using an insulating material to create an alternating compartment of three materials. To accommodate the changes in compressor outlets at all levels, the phase-transition temperature decreases from PCM1 to PCM3, allowing heat energy to be stored at different temperatures. It shows that the system can not only capture heat energy in different temperature ranges but also store the fluctuating energy generated by the external compressor outlets and electric heaters in the form of latent heat and output it in the form of stable heat energy in the energy release stage.

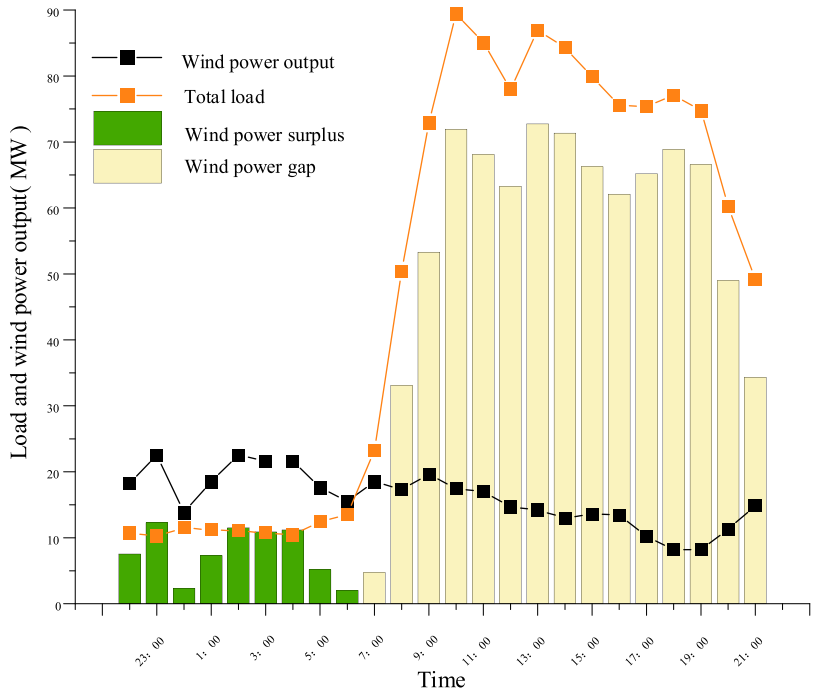

FIGURE 4
Typical daily hourly load of a port in summer.

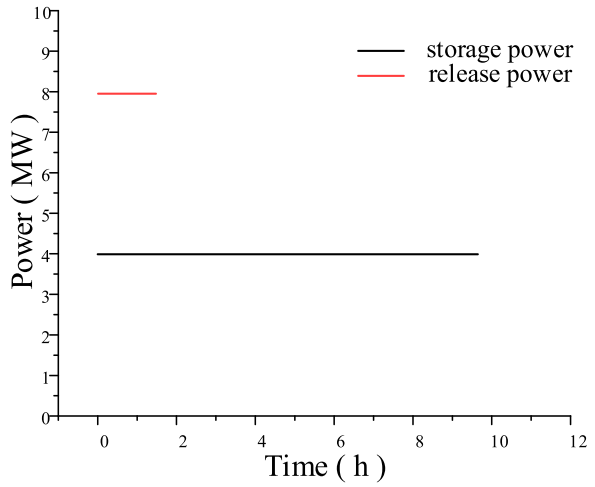

FIGURE 5
Energy storage/release characteristics of a constant-pressure adiabatic compressed air energy storage system.

4.2 System operating mode

The calculation process is shown in Figure 3. During the compression process, the wind power output W_{wind} is allocated according to the operating power range of the compressor and the electric heater. When W_{wind} exceeds the upper limit of compressor power W_{cH}, the excess part W_{heat} is used to heat the PCM after judgment, and the remaining part drives the compressor to store energy. When W_{wind} is located between W_{cH} and W_{cL}, the compressor is directly driven to store energy, and the electric heater is not started. When W_{wind} is lower than W_{cL}, the electric heater is started to heat the PCM, and the compressor is not started. At the end of the compression process, the electrical power E_c and thermal power H_c of the energy storage section of the CPCM-IA-CAES system are obtained through the given initial conditions of the system, such as the inlet pressure and temperature of the compressor.

During the turbine process, the system consistently releases energy due to the constant temperature of the PCM, which supports the stable release of energy. After the turbine releases all the air, it is assessed for the presence of residual heat in the PCM. If present, it is used to heat the heat load according to the principle of temperature matching. Finally, the electric power E_e and thermal power H_e of the energy release section are output.

To simplify the calculation, it is assumed that 1) air is regarded as ideal air, and its specific heat capacity is regarded as a constant; 2) the heat transfer fluid pump loss is ignored; and 3) the heat loss in the pipeline is also ignored.

5 Case analysis

5.1 Energy storage system configuration scheme and system characteristics

The hourly load and wind power of a large port on a typical summer day in China are shown in Figure 4 (Song et al., 2020). The total wind power generation in a day is 243,446.88 kW h. The port electricity gap period is from 7: 00 to 21: 00, the maximum power gap is approximately 72.739 MW, the power surplus period is from

TABLE 1 Basic parameters of a typical compressed air energy storage system.

Parameter	Value	Parameter	Value
Heat exchanger efficiency	0.9	Air reservoir volume/m^3	4,000
Compressor efficiency	0.9	Expander efficiency	0.9
Total compressor power/kW	3,990.65	Total power of the expander/kW	7,949.8
System efficiency/%	65.96	Energy density/(kW·h·m^{-3})	8.7
Compressor starting power/kW	2,777.71	—	—

22: 00 to 6: 00 on the next day, and the maximum power surplus is approximately 12.294 MW.

To alleviate the power fluctuation at the port, it is proposed to configure the energy storage device. The specific scheme is as follows:

1) Scheme 1: The IA-CAES system is configured, and its energy storage/release power characteristics (Wang et al., 2016a) are shown in Figure 5. The design parameters are shown in Table 1. The energy storage/release process of the IA-CAES system runs under sliding pressure. According to the power fluctuation of the system, three sets of the constant pressure adiabatic system are configured (Yongpeng et al., 2023). The energy storage is started from 22: 00 to 6: 00, and the energy release is started at 7: 00. The three sets of systems release energy in turn.

In the energy storage process of the IA-CAES system, the compressor operates under sliding pressure, and the energy storage power is determined by the pressure of the air storage reservoir, which is not adjustable, and the energy storage power is maintained at 3,990.65 kW. This feature makes the IA-CAES system alone unable to cope with the fluctuating energy storage power demand. In the process of energy release, due to the smooth pressure operation, the energy release power is determined by the pressure of the air storage reservoir and cannot be adjusted. In the process of energy release, the pressure of the air storage reservoir is constant, and the energy release power is maintained at 7,949.8 kw.

2) Scheme 2: The CPCM-IA-CAES system is configured, and its design parameters are shown in Tables 2–4 (Zhang et al., 2019). The energy storage/release characteristic is shown in Figure 6.

When the conventional IA-CAES system is in energy storage, its working condition is adjusted according to the input power. As shown in Figure 5, when the electric power is less than the starting power of the compressor, the electric heater starts and stores the electric energy in the form of thermal energy. The energy storage power range of Case 2 is theoretically 0–12,000 kW.

The design parameters of the IA-CAES and CPCM-IA-CAES systems are compared. When the environmental parameters and some key design parameters (compressor and trans-equal entropy efficiency) are the same, the total design energy storage power is similar (Scheme 1 is 11.972 MW and Scheme 2 is 12 MW):

1) The latter has higher system efficiency because it realizes cascade energy utilization and independent supply and reduces energy loss in the process of energy storage/release.
2) The energy storage density of the latter is higher than that of the former because, in the face of fluctuating input power, the latter can collect more abandoned wind, while the former has a small power adjustment range, resulting in a large amount of energy loss.
3) The energy storage power range of the latter can be actively adjusted, and the energy storage range is greater than that of the former.

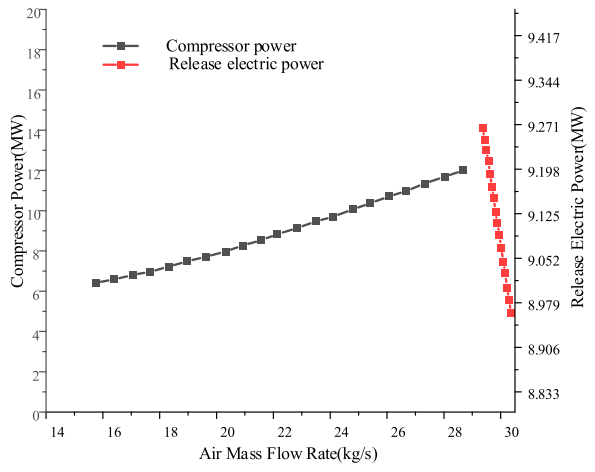

FIGURE 6
Energy storage/release characteristics.

5.2 Comparison of the energy storage/release process of different schemes

Figure 7 shows the energy storage process of Schemes 1 and 2. The energy storage process of Scheme 1 is similar to that of Scheme 2 at 22:00 and 1:00–5:00, and both schemes can absorb surplus energy at this time. At 0:00 and 6:00, the wind power is 2.33 and 2.02 MW, respectively, which is less than the minimum starting power of the compressor. Therefore, Scheme 1 has a wind curtailment at these two moments. Due to the configuration of the electric heater, Scheme 2 can store these two parts of the waste energy in the form of thermal energy in the PCM.

At 23:00, the wind power is 12.234 MW, which is greater than the maximum energy storage power of Scheme 1, so Scheme 1 has

TABLE 2 Basic parameters of the CPCM-IA-CAES system.

Parameter	Value	Parameter	Value
Ambient temperature/K	298	Ambient pressure/MPa	0.1
Compression/expansion stage	3	Maximum volume of air storage reservoir/m^3	7,248.51
Pressure of the air storage reservoir/MPa	8	Temperature of the air storage reservoir/K	303
Maximum energy storage power/kW	12,000	Energy density/(kW·h·m^{-3})	9.8911
Energy storage time/h	8	System efficiency/%	74.68
Release time/h	8	—	—

TABLE 3 Basic parameters of compression and expansion sections.

Parameter	Value	Parameter	Value
Compression ratio	4.0122	Expansion ratio	3.8059
Compressor efficiency	0.84	Expander efficiency	0.88
Mass flow rate of the compressor/(kg/s)	15.1816	Mass flow rate/(kg·s^{-1})	30.361
Pressure loss of each intercooler/MPa	0.02	Pressure loss of each reheater/MPa	0.02
Compressor starting power/kW	6,415.33	Total power of turbine/kW	8,961.98

TABLE 4 Basic parameters of the CPCM-IA-CAES system.

Number	Density (kg/m3)	Latent heat (kJ/kg)	Melting temperature (K)
PCM1	2,370	142	469
PCM2	1976	80.7	433
PCM3	1,455	168	395

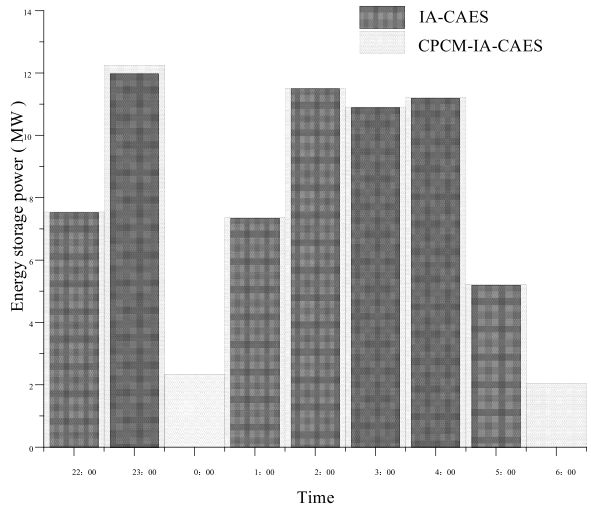

FIGURE 7
Charge/discharge process of Schemes 1 and 2.

abandoned wind at this time. At this time, Scheme 2 compressor and electric heater work, at the same time, through the air storage reservoir and PCM common energy storage, collecting and utilizing the abandoned wind power loss of scheme 1. However, when wind power is greater than the maximum power of the compressor and the electric heater running at the same time, there is still wind curtailment, and there is still room for optimization in the system capacity design and operation method of Scheme 2.

5.3 Comprehensive performance comparison of different energy storage schemes

Compared with Scheme 1, Scheme 2 can effectively reduce the abandoned wind power. For Scheme 1, at 22:00 and 1:00–5:00, wind power is more matched with the system energy storage power, and the abandoned wind power is less; in other moments, the matching is not good, and the abandoned wind power is large. In Scheme 2, if the wind power exceeds the maximum power range of the simultaneous operation of the compressor and the electric heater, there is still wind abandonment.

The total abandoned wind power, abandoned wind rate, system efficiency, and energy storage density of each scheme are shown in Table 5. Scheme 2 can actively adjust the energy storage power and use the excess electricity for energy storage, so the abandoned wind

TABLE 5 Comprehensive performance comparison of different schemes.

Parameter	Scheme 1	Scheme 2
Total abandoned wind power/(kW· h)	4,644.46	0.00
Abandoned wind rate/%	5.7	0.00
System efficiency/%	65.96	74.68
Energy density/(kW·h·m^{-3})	8.6940	9.8911

rate and abandoned wind power of Scheme 2 are significantly lower than those of Scheme 1.

Since the energy storage/release process of the IA-CAES system belongs to its characteristics and cannot be adjusted, the energy storage/release performance of Scheme 1 is the same as its design performance (Table 1). By integrating three sets of IA-CAES systems with small designed energy storage power, it has a certain ability to cope with fluctuating residual power; however, the ability to cope with deviation from the "ladder" type of fluctuating residual power input is still poor. At the same time, the complexity of the system increases, and the cost of system construction and maintenance is high (Liu et al., 2016).

The CPCM-IA-CAES system often deviates from the design operating point of the system, and its actual performance is slightly deviated from the design performance, as shown in Tables 2, 3. Compared with the system design parameters of Scheme 1, the cycle efficiency of Scheme 2 is improved. The reason is that heat storage at all levels of Scheme 1 is used in energy release after mixing. Scheme 2 uses independent heat storage and heat consumption of compressors and expanders at all levels to ensure the correspondence between compressors and expanders at each level, and strong correspondence will make the system more efficient. The energy storage density of Scheme 2 is higher than that of Scheme 1 because the configuration of the electric heater increases the energy storage power range of Scheme 2, which has clear advantages in the face of power fluctuation and increases the energy storage density of Scheme 2.

By comprehensively comparing the two energy storage schemes, Scheme 1 has insufficient ability to deal with fluctuating energy storage power, and the system is complex, which is not suitable for dealing with wind power fluctuations. Scheme 2 has a wider range of energy storage power regulations and a higher efficiency of the heat storage process due to the configuration of independent phase-change heat storage and an electric heater, which can effectively cope with the fluctuation of renewable energy.

Comprehensive performance comparisons of related research systems are shown in Table 6. Because the CPCM-IA-CAES system can regulate storage power and use abandoned wind power for energy storage, its storage power regulation index is 16.67% higher than that of the underwater compressed air energy storage (UW-CAES) system. The variable configuration adiabatic compressed air energy storage (VCAES) system has a higher storage power index (87.17%), but it has two sets of compression and expansion components, and its structural complexity is higher than that of CPCM-IA-CAES, which reduces its operability. The system efficiency of the UW-CAES system is 65.96%, which is lower than that of CPCM-IA-CAES because the heat storage at each stage of the UW-CAES is mixed and deposited into the heat storage device before releasing the energy for use, and the loss of heat leads to the low efficiency of the system, whereas the CPCM-IA-CAES system adopts step-independent heat storage, i.e., each stage of the compressor and expander independently stores and uses heat, and this new approach ensures that each stage of the compressor and expander independently stores and uses heat. This new method can ensure the correspondence between each compressor and expander, and the strong correspondence will make the system more efficient.

6 Conclusion

1) Aiming at the problem that the current IA-CAES system is limited by the energy loss in the energy storage stage and that the system is difficult to operate efficiently, this paper combines the typical compressor/turbine characteristic and the typical constant-pressure air storage reservoir characteristics and proposes a cascade phase-change independent heat storage adiabatic CAES cogeneration system design method and its operating rules.
2) By constructing the energy storage characteristic curves and energy release characteristic curves of the IA-CAES and CPCM-IA-CAES systems, the complete CPCM-IA-CAES system storage/release variable operating condition model is established. The results show that the designed system realizes efficient utilization of waste energy, the system efficiency is increased from 65.96% to 74.68%, and the energy storage density is increased from 8.69 to 9.89 kW h m^{-3}.
3) The case study compares the storage/release performance and overall performance of the IA-CAES and CPCM-IA-CAES systems, and the results show that the CPCM-IA-CAES system has an advantage in coping with the fluctuation of input power. The wind abandonment rate is reduced by 5.7%, 4,644.46 kW h of abandoned wind power is recovered, and the energy storage power index is increased by 16.67% compared with IA-CAES.

TABLE 6 Performance comparison of related systems.

Parameter	UW-CAES	VC-ACAES	CPCM-IA-CAES
Number of compression expansion components/group	1	2	1
Energy storage power index/%	83.33	87.17	100
System efficiency/%	65.96	60.79	74.68
Energy storage density/(kW h m^{-3})	8.6940	—	9.8911

In this paper, the analysis of the variable operating condition performance of the CPCM-IA-CAES system is conducted based on the assumption of steady-state operation. However, the operation or regulation of variable operating conditions in actual engineering is a dynamic process, and it is of great significance to further study the influence of the dynamic characteristics of the system on the performance under variable operating conditions.

Data availability statement

The original contributions presented in the study are included in the article/Supplementary Material; further inquiries can be directed to the corresponding author.

Author contributions

KW: writing–original draft. LC: writing–review and editing. XL: writing–review and editing. CZ: writing–review and editing.

Funding

The author(s) declare that financial support was received for the research, authorship, and/or publication of this article. This work was supported by the Joint Funds of the National Natural Science Foundation of China (U22A20224).

Conflict of interest

The authors declare that the research was conducted in the absence of any commercial or financial relationships that could be construed as a potential conflict of interest.

Publisher's note

References

Arabkoohsar, A., Rahrabi, H., Alsagri, A., and Alrobaian, A. (2020). Impact of Off-design operation on the effectiveness of a low-temperature compressed air energy storage system. *Energy* 197, 117176. doi:10.1016/j.energy.2020.117176

Budt, M., Wolf, D., Span, R., and Yan, J. (2016). A review on compressed air energy storage: basic principles, past milestones and recent developments. *Appl. energy* 170, 250–268. may 15. doi:10.1016/j.apenergy.2016.02.108

Erdiwansyah, M., Husin, H., and Zaki, M., (2021). A critical review of the integration of renewable energy sources with various technologies. *Prot. Control Mod. Power Syst.* 6 (1), 3. doi:10.1186/s41601-021-00181-3

Guo, C., Xu, Y., Zhang, X., Guo, H., Zhou, X., Liu, C., et al. (2017). Performance analysis of compressed air energy storage systems considering dynamic characteristics of compressed air storage. *Energy* 135, 876–888. doi:10.1016/j.energy.2017.06.145

He, Q., Li, G., Lu, C., Du, D., and Liu, W. (2019). A compressed air energy storage system with variable pressure ratio and its operation control. *Energy* 169, 881–894. doi:10.1016/j.energy.2018.12.108

Li, J., Li, X., Wei, F., Yan, P., Liu, J., and Yu, D. (2023a). Research on techno-economic evaluation of new type compressed air energy storage coupled with thermal power unit. *Proc. CSEE*, 1–13. doi:10.13334/j.0258-8013.pcsee.222819

Li, J., Liang, C., Zhang, Z., Liang, Z., and Yang, H. (2023b). Analysis of energy storage policies and business models in new power system. *High. Volt. Appar.* 59 (07), 104–116. doi:10.13296/j.1001-1609.hva.2023.07.012

Li, R., Wang, H., and Zhang, H. (2019). Dynamic simulation of a cooling, heating and power system based on adiabatic compressed air energy storage. *Renew. Energy* 138, 326–339. AUG. doi:10.1016/j.renene.2019.01.086

Liu, Y., Qiu, X., Qiu, G., Tang, K., Yan, T., and Wan, C. (2016). Multi-agent game model of micro-grid containing energy storage system in islanding operation. *High. Volt. Appar.* 52 (07), 75–81. doi:10.13296/j.1001-1609.hva.2016.07.012

Luo, X., Wang, J., Dooner, M., and Clarke, J. (2015). Overview of current development in electrical energy storage technologies and the application potential in power system operation. *Appl. energy* 137, 511–536. 137-Jan.1. doi:10.1016/j.apenergy.2014.09.081

Mazloum, Y., Sayah, H., and Nemer, M. (2017). Dynamic modeling and simulation of an isobaric adiabatic compressed air energy storage (IA-CAES) system. *J. Energy Storage* 11, 178–190. JUN. doi:10.1016/j.est.2017.03.006

Mei, S., Li, R., Chen, L., and Xue, X. (2018). An overview and outlook on advanced adiabatic compressed air energy storage technique. *Proc. CSEE* 38 (10), 2893–3140. doi:10.13334/j.0258-8013.pcsee.172138

Nantian, H., Qingzhu, C., Guowei, C., Dianguo, X., Liang, Z., and Wenguang, Z. (2020). Fault diagnosis of bearing in wind turbine gearbox under actual operating conditions driven by limited data with noise labels. *IEEE Trans. Instrum. Meas.* (99), 1. doi:10.1109/TIM.2020.3025396

Olujobi, O. J. (2020). The legal sustainability of energy substitution in Nigeria's electric power sector: renewable energy as alternative. *Prot. Control Mod. Power Syst.* 5 (32), 32–12. doi:10.1186/s41601-020-00179-3

Rahbari, H. R., and Arabkoohsar, A. (2021). A thorough investigation of the impacts of trigeneration-CAES off-design operation on its thermodynamics, economic and environmental effectiveness. *Sustain. Energy Technol. Assessments* 44, 101024. doi:10.1016/j.seta.2021.101024

Ruiheng, L., Dong, X., Hao, T. a., and Yiping, Z. (2023). Multi-objective study and optimization of a solar-boosted geothermal flash cycle integrated into an innovative combined power and desalinated water production process: application of a case study. *Energy* 282, 128706. doi:10.1016/j.energy.2023.128706

Sciacovelli, Y., Chen, H., Yt, W., Jh, G., Wang, J., Garvey, S., et al. (2017). Dynamic simulation of Adiabatic Compressed Air Energy Storage (A-CAES) plant with integrated thermal storage - link between components performance and plant performance. *Appl. Energy* 185 (-), 16–28. doi:10.1016/j.apenergy.2016.10.058

Shafiee, S., Zareipour, H., and Knight, A. M. (2018). Considering thermodynamic characteristics of a CAES facility in self-scheduling in energy and reserve markets. *IEEE Trans. Smart Grid* 9 (4), 3476–3485. doi:10.1109/tsg.2016.2633280

Shang, C., Rahbarib, H. R., Arabkoohsarc, A., and Tong, Z. (2020). Impacts of partial-load service on energy, exergy, environmental and economic performances of low-temperature compressed air energy storage system. *J. Energy Storage* 32, 01–18. doi:10.1016/j.est.2020.101900

Shu, G., Li, X., Tian, H., Liang, X., Wei, H., and Wang, X. (2014). Alkanes as working fluids for high-temperature exhaust heat recovery of diesel engine using organic Rankine cycle. *Appl. Energy* 119 (1), 204–217. doi:10.1016/j.apenergy.2013.12.056

Song, T., Li, Y., Zhang, X. P., Wu, C., Gu, H., Guo, Y., et al. (2020). Integrated port energy system considering integrated demand response and energy interconnection. *Int. J. Electr. Power Energy Syst.* 117, 105654. doi:10.1016/j.ijepes.2019.105654

Tessier, M. J., Floros, M. C., Bouzidi, L., Narine, S. S., Lund, H., and Kaiser, M. J. (2016). Exergy analysis of an adiabatic compressed air energy storage system using a cascade of phase change materials. *Energy* 106, 528–534. doi:10.1016/j.energy.2016.03.042

Tong, Z., Cheng, Z., and Tong, S. (2021). A review on the development of compressed air energy storage in China: technical and economic challenges to commercialization. *Renew. Sustain. Energy Rev.* 135, 110178. doi:10.1016/j.rser.2020.110178

Wang, Z., Xiong, W., David, S.-K. T., Rupp, C., and Wang, Z. (2016a). Conventional and advanced exergy analyses of an underwater compressed air energy storage system. *Appl. Energy* 180, 810–822. doi:10.1016/j.apenergy.2016.08.014

Wang, Z., Xiong, W., Wang, H., and Wang, Z. (2016b). Exergy analysis of the pneumatic line throwing system. *Int. J. Exergy* 19 (3), 364. doi:10.1504/IJEX.2016.075669

Xiao, M., Yang, C., Xiao, R., Xie, G., and Ma, X. (2023). Design on isobaric adiabatic compressed air energy storage system for unstable input at power source-side. *Proc. CSEE* 43 (06), 2168–2179. doi:10.13334/j.0258-8013.pcsee.222504

Xu, P., Fu, W., Lu, Q., Zhang, S., Wang, R., and Meng, J. (2023). Stability analysis of hydro-turbine governing system with sloping ceiling tailrace tunnel and upstream surge tank considering nonlinear hydro-turbine characteristics. *Renew. Energy* 210, 556–574. doi:10.1016/j.renene.2023.04.028

Xu, Y., Chen, H., Liu, J., and Tan, C. (2012). Performance analysis on an integrated system of compressed air energy storage and electricity production with wind-solar complementary method. *Proc. CSEE* 32 (20), 88–95+144. doi:10.13334/j.0258-8013.pcsee.2012.20.020

Xuezhao, Z., Guobin, C., Jun, G., Wenjing, G., Yuan, H., and Xin, T. (2023). Combustion characteristics and thermal decomposition mechanism of the flame-retardant cable in urban utility tunnel. *Case Stud. Therm. Eng.* 44, 102887. doi:10.1016/j.csite.2023.102887

Yang, N., Dong, Z., Wu, L., Zhang, L., Shen, X., Chen, D., et al. (2022a). A comprehensive review of security-constrained unit commitment. *J. Mod. Power Syst. Clean Energy* 10 (3), 562–576. doi:10.35833/mpce.2021.000255

Yang, N., Qin, T., Wu, L., Huang, Y., Huang, Y., Xing, C., et al. (2022b). A multi-agent game based joint planning approach for electricity-gas integrated energy systems considering wind power uncertainty. *Electr. Power Syst. Res.* 204, 107673. doi:10.1016/j.epsr.2021.107673

Yang, N., Yang, C., Xing, C., Ye, D., Jia, J., Chen, D., et al. (2021). Deep learning-based SCUC decision-making: an intelligent data-driven approach with self-learning capabilities. *IET Generation, Transm. Distribution(Wiley-Blackwell)* 16, 629–640. doi:10.1049/gtd2.12315

Yang, Y., Qin, C., Zeng, Y., and Wang, C. (2022c). Optimal coordinated bidding strategy of wind and solar system with energy storage in day-ahead market. *J. Mod. Power Syst. Clean Energy* 10 (1), 192–203. doi:10.35833/mpce.2020.000037

Yongpeng, S., Junchao, X., Ting, H., Lei, Y., and Yanqiu, X. (2023). CEEMD-Fuzzy control energy management of hybrid energy storage systems in electric vehicles. *IEEE Trans. Energy Convers.*, 1–12. doi:10.1109/TEC.2023.3306804

Zhang, Na, and Cai, R. (2002a). Analytical solutions and typical characteristics of part-load performances of single shaft gas turbine and its cogeneration. *Energy Convers. Manag.* 43 (9-12), 1323–1337. doi:10.1016/s0196-8904(02)00018-3

Zhang, N., and Cai, R. (2002b). Analytical solutions and typical characteristics of part-load performances of single shaft gas turbine and its cogeneration. *Energy Convers. Manag.* 43 (9-12), 1323–1337. doi:10.1016/S0196-8904(02)00018-3

Zhang, N., Lin, R., and Cai, R. (1996). General formulas for axial compressor performance estimation. *J. Eng. Thermophys.* (01), 21–24.

Zhang, Y., Xu, Y., Zhou, X., Guo, H., Zhang, X., and Chen, H. (2019). Compressed air energy storage system with variable configuration for accommodating large-amplitude wind power fluctuation. *Appl. Energy* 239, 957–968. APR.1. doi:10.1016/j.apenergy.2019.01.250

Zhou, Q., Sun, Y., Lu, H., and Wang, K. (2022). Learning-based green workload placement for energy internet in smart cities. *J. Mod. Power Syst. Clean Energy* 10 (1), 91–99. doi:10.35833/mpce.2020.000271

Nomenclature

CAES	Compressed air energy storage
IA-CAES	Isobaric adiabatic compressed air energy storage
PCM	Phase-change material
CPCM-IA-CAES	Isobaric adiabatic compressed air energy storage system using a cascade of phase-change materials
η	Isentropic efficiency
V	Volume
E	Exergy
G	Mass flow rate
h	Specific enthalpy of air
$\dot{m}$	Reduced mass flow rate
$\dot{n}$	Reduced rotating speed
W	Power
T	Temperature
i	Specific enthalpy of fluid
ρ	Density
c_p	Specific heat at constant pressure
π	Expansion ratio
p	Pressure
Q	Thermal energy
U	Heat transfer coefficient
A	Heat transfer area
c	Compressor
0	Design point
t	Turbine
s	Isentropic process
in	Inlet
out	Outlet
$wind$	Wind power
H	Upper limit
L	Lower limit